Synthesis and Characterization of Model Cyclic Block Copolymers of Styrene and Butadiene. Comparison of the Aggregation Phenomena in Selective Solvents with Linear Diblock and Triblock Analogues

Hermis Iatrou and Nikos Hadjichristidis*

Department of Chemistry, University of Athens, Panepistimiopolis, 15771 Athens, Greece

Gerd Meier, Henrich Frielinghaus, and Michael Monkenbusch

Institut für Festkörperforschung, Forscunszentrum Jülich GmbH, D-52425 Jülich, Germany

Received December 11, 2001; Revised Manuscript Received April 1, 2002

ABSTRACT: The synthesis and characterization of model cyclic diblock copolymers of styrene (St) or perdeuterated styrene (St-d_8) and butadiene (Bd) are presented. Since conventional methods of characterization cannot separate completely the cyclic copolymer from its linear precursor, differences in the micellar behavior were used as a method for investigation of their purity. For this purpose, in addition to the cyclic and linear triblock copolymers, two linear diblocks with similar compositions, and molecular weight equal or half of the cyclic diblocks, were also synthesized. The synthetic approach of the cyclics involved the reaction of (1,3-phenylene)bis(3-methyl-1-phenylpentylidene)dilithium initiator with butadiene in the presence of *sec*-BuOLi, followed by polymerization of St (or St-d_8). The cyclization of the resulting α,ω-difunctional triblock copolymer was performed by using bis(dimethylchlorosilyl)-ethane, under high dilution conditions. The copolymers were characterized by size exclusion chromatography, membrane osmometry, NMR and UV spectrometry, and viscometry. The micelles formed in the selective solvents *n*-decane (for PBd) and dimethylformamide (for PS-d_8) were characterized by small-angle neutron scattering and dynamic light scattering. It was found that the aggregation number of the cyclic copolymers was the smallest among the different macromolecular architectures. Moreover, the SANS data for the triblocks in *n*-decane indicated the presence of 37% dangling chains which did not appear in the data for the corresponding cyclic copolymers. Considering that 5% of dangling chains is possible to be detected, it proves that the cyclic copolymers are at least 87% pure. A scaling model was used in order to justify the difference in the aggregation numbers between the four different copolymers.

1. Introduction

Since the discovery in 1962[1] that certain DNA molecules occur in nature in a closed loop form, many attempts have been made to synthesize well-defined macromolecular cyclic polymers.[2−10] Due to the absence of free chain ends, the monomeric units of cyclic homopolymers are equivalent. Moreover due to the cyclic form of the molecules, the intramolecular interactions are increased, compared to a linear analogue. As a consequence, in dilute solution, the second virial coefficient, the dimensions, and the intrinsic viscosity[2−3,11] are reduced. In bulk, the cyclic architecture influences the glass transition temperature (T_g) of homopolymers, the morphology,[8] and the order−disorder transition of the copolymers.[12] The above characteristics make the cyclic macromolecules very interesting.

Two general synthetic approaches have been reported up to now, based either on a α,ω-homodifunctional or α,ω-heterodifunctional polymeric chains. In the first case the cyclization requires a difunctional coupling agent, while in the second the cyclization requires some type of activation for the intramolecular reaction. Although a large variety of different functional groups has been used for the synthesis of cyclic homo- and copolymers, the purity of the final products are always in question, since only limited separation methods can separate completely cyclic homopolymer from the linear precursor.[13] In the case of cyclic copolymers, no analytical method has been presented so far. Moreover, as far as we know, only one complete series of macrocyclic diblock copolymers of styrene and dimethylsiloxanes has been prepared by Hogen-Esch and Yin.[8]

Diblock copolymers in a selective solvent exhibit surfactant-like behavior, and their study can enhance the understanding of the relation between molecular structure and properties such as detergency, surfactancy, colloidal dispersion, and stabilization. Although many studies have been presented on the micellar behavior of block copolymers in a selective solvent,[14−21] only a few compare the micellar characteristics of copolymers exhibiting different macromolecular architectures but similar molecular weight and composition.[22−26] Booth et al.[26] presented the synthesis and micellar behavior of cyclic block copolymers of poly(ethylene oxide) and propylene oxide in water. They compared the aggregation numbers and dimensions of these copolymers with the triblock precursors and the linear diblock analogues.

In this work the synthesis and characterization of a series of cyclic polystyrene (PS) (or perdeuterated polystyrene, PS-d_8)-*b*-polybutadiene (PBd) copolymers with a PS fraction ranging from 15 to 70% (w/w) is presented. Moreover, the synthesis of the linear triblock PS (or PS-d_8)-*b*-PBd-*b*-PS and (PS-d_8)-*b*-PBd analogues with either the same molecular weight and composition (for the case of the triblocks and diblocks) or half the molecular weight but similar composition (for the case of diblocks) is also presented. All block copolymers have been characterized by SEC, UV spectrometry, viscom-

* To whom correspondence should be addressed, e-mail: hadjichristidis@chem.uoa.gr.

10.1021/ma0121565 CCC: $22.00
Published on Web 06/04/2002

Scheme 1

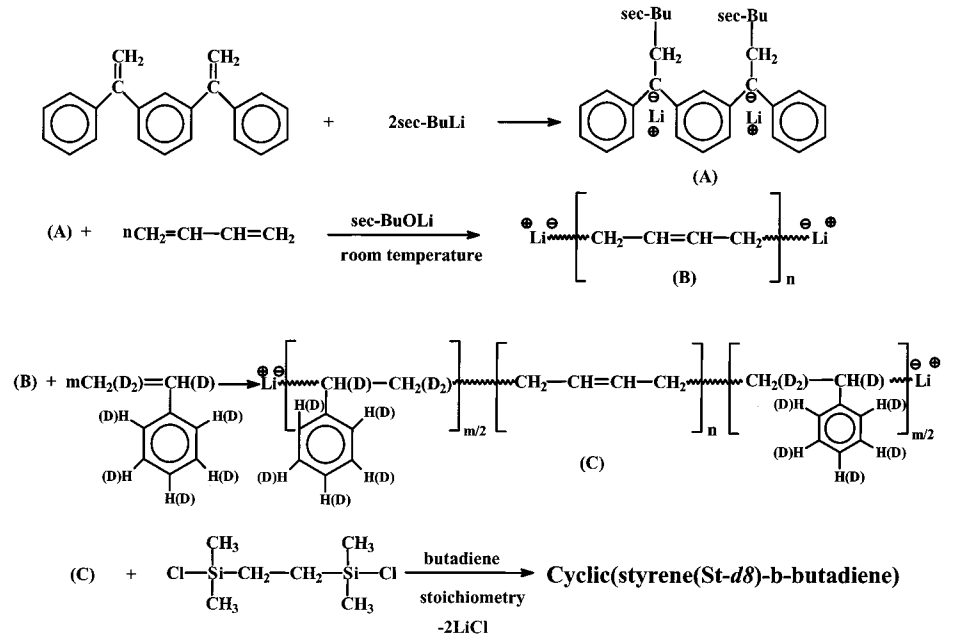

etry, and membrane osmometry. Since these analytical methods are not sufficient to determine the purity of cyclic copolymers, the micellar behavior of the linear analogues was examined and compared with the behavior of the cyclics.

The molecular characteristics of the micelles were obtained by using small-angle neutron scattering (SANS) and dynamic light scattering (DLS) in *n*-decane and *N,N*-dimethylformamide (DMF). *n*-Decane is a selective solvent for PBd, while DMF is a selective solvent for PS or PS-d_8. By using mixtures of deuterated and protonated solvents it was possible, in most cases, to match exactly either the corona (shell) or the core of the micelle and measure separately the structural properties of each component by SANS. The influence of the macromolecular architecture on the micellar behavior is also investigated, by comparing the dimensions of the micelles formed by the linear analogues and the cyclic block copolymer, of one composition, in two different solvents.

Finally, the experimental observations are discussed in terms of scaling models. The discussion is based upon the differentiation of the free energy of the micelles according to the macromolecular architecture; i.e., the formation of loops in the core or the corona of the micelle introduces an entropic penalty to the free energy of the micelle, compared to the corresponding linear diblock copolymer.

2. Experimental Section

Synthesis of the Copolymers. Styrene (99%), styrene-d_8 (98 atom %), butadiene (99%), *n*-butyllithium (1.6 M) in hexanes, bis(dimethylchlorosilyl)ethane (BDCSE) (98%), benzene (99%), *n*-decane (99%), DMF (99%), *n*-decane-d_{22} (99 atom % D) and DMF-d_7 (99 atom % D) were purchased from Aldrich. Purification of monomers and solvents to the standards required for anionic polymerization has been described in detail elsewhere.[27] Methyllithium (Aldrich), triphenyl methylphosphonium iodide (98% Alpha) and 1,3-bis(1-phenone) benzene (PBOP) (98%, Aldrich), were used for the preparation of 1,3-bis(1-phenylethenyl)-benzene (PEB) according to the method of Ignatz-Hoover.[28] *sec*-Butyllithium (*sec*-BuLi) and *sec*-butoxylithium (*sec*-BuOLi) were prepared in vacuo either from *sec*-butyl chloride or *sec*-butanol and lithium dispersion, respectively. *sec*-BuLi was used as the activator of PEB, for the preparation of (1,3-phenylene)bis(3-methyl-1-phenylpentylidene)dilithium initiator (DLI).

Scheme 2

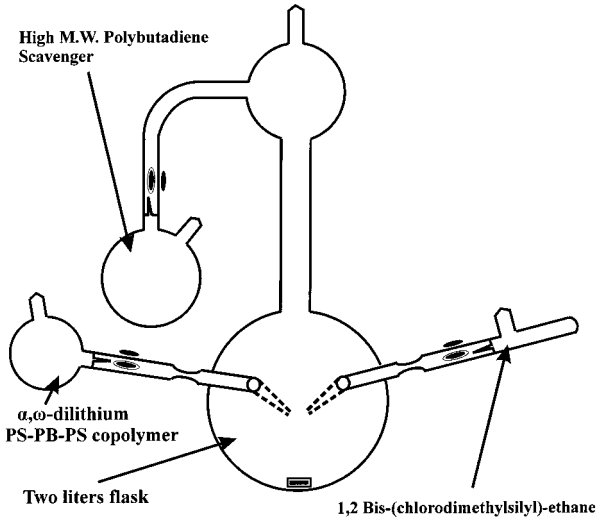

The basic reactions used for the synthesis of the cyclic copolymers are shown in Scheme 1.

A 5% solution (w/v) of an α,ω-difunctional PBd homopolymer in benzene was synthesized by the sequential addition of *sec*-BuOLi and butadiene to the DLI solution. The molar ratio of *sec*-BuOLi/C−Li was 4/1. The polymerization of Bd took place at 20 °C for 6 days. Then a small aliquot was removed for characterization and the appropriate amount of St (or St-d_8) was added. It was found that about 1 h was required for the crossover reaction and the polymerization was required three more days to reach completion. Then a small amount of butadiene was added in order to introduce three to four units of Bd at each living end. Part of the resulted α,ω-difunctional PS-*b*-PBd-*b*-PS triblock copolymer was neutralized by degassed methanol (MeOH) and the rest was inserted in an ampule equipped with a break-seal for the cyclization reaction.

The reactor used for the cyclization reaction is shown in Scheme 2.

The two ampules were attached in a way that each reactant could be added separately. Prior the cyclization reaction, the reactor was purged with a solution of *n*-BuLi in benzene. The

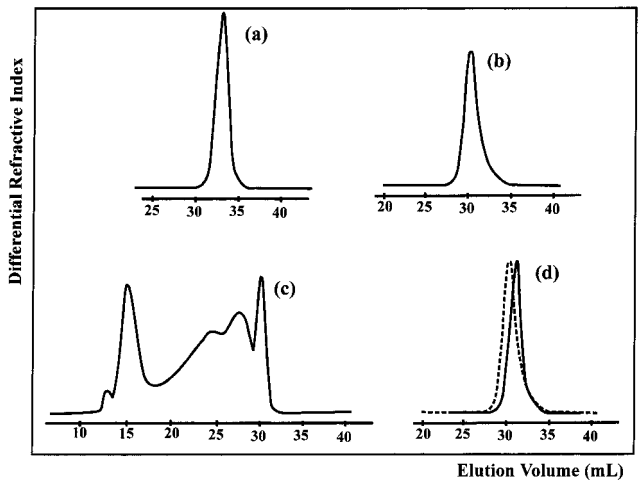

Figure 1. SEC chromatograms during the synthesis of the cyclic copolymer C22−28: (a) PBd homopolymer; (b) (PS-d_8)-*b*-PBd-*b*-(PS-d_8) triblock copolymer; (c) reaction products after the cyclization reaction and addition of the high molecular weight PBd chain; (d) fractionated cyclic copolymer; dotted line: linear precursor (b).

Table 1. Molecular Characteristics of the Cyclic Copolymers and the Linear Precursors

sample	M_n(PBd) × 10^3 [b]	M_n(triblock) × 10^3 [b]	M_w/M_n (triblock)[c]	M_n(cyclic) × 10^3 [b]	M_w/M_n (cyclic)[c]
C45−5	42.0	47.5	1.06	47.2	1.06
C40−20	41.5	55.9	1.07	56.5	1.07
C28−22[a]	32.0	55.1	1.08	53.5	1.09
C22−28[a]	23.0	53.0	1.10	53.4	1.11
C15−35[a]	16.1	56.9	1.15	58.0	1.16

[a] Polystyrene block is perdeuterated. [b] Membrane osmometry in toluene at 37 °C. [c] Size exclusion chromatography in THF at 25 °C.

Table 2. Composition of the Cyclic Copolymers and the Linear Precursors

sample	% PS from M_n (w/w)	% PS (w/w) by NMR (triblocks)	% PS (w/w) by NMR (cyclics)	% PS (w/w) by UV (triblocks)	% PS (w/w) by UV (cyclics)
C45−5	12	12	14	14	15
C40−20	26	28	29	30	32
C28−22	42	*a*	*a*	43	44
C22−28	56	*a*	*a*	54	55
C15−35	72	*a*	*a*	70	73

[a] N/A, deuterated polystyrene.

procedure of the addition of the living chains and the linking agent was as follows: 3−5 mL of the 5% solution was diluted into 1.6 L of solvent, followed by the addition of a stoichiometric amount of linking agent. The reagents were left to react for 20 min, and the procedure was repeated until all living chains were inserted into the reactor. The addition was performed in many steps over about 3 days. After the completion of the addition, the reaction mixture was left for another 3 days to react completely, and a slight excess of linking agent (∼10% mol/mol) was introduced. Then a large amount of high molecular weight PBd living polymer (∼200 kg/mol) was introduced in a molar ratio of living ends [PBdLi]/[LiPS−PBd-PSLi] equal to 1:1. The reaction mixture was left for another 7 days, the reactor was opened, and the reaction mixture was fractionated by using toluene/MeOH as the solvent/nonsolvent pair. The synthetic procedure as well as the fractionation was monitored by SEC. A typical example is given in Figure 1.

The total molecular weight of the triblock precursors (and the cyclics) was approximately between 47 and 57 kg/mol. The molecular characteristics are shown in Tables 1 and 2.

Table 3. Molecular and Compositional Characteristics of the Diblock Analogues of the C22−28 Samples

sample	M_n(PS-d_8) × 10^{3a}	M_n(diblock) × 10^{3a}	% PS-d_8 from M_n	$I = M_w/M_n$	% PS-d_8 by UV
D22−28	23.2	44.0	52	1.03	54
(D22−28)/2	14.0	26.0	54	1.03	56

[a] Membrane osmometry in toluene at 37 °C.

Table 4. Viscosity Measurements of the Triblock Copolymers and the Corresponding Cyclics, in Toluene at 30 °C

	triblock		diblock	
sample	$[\eta]$ (mL/g)	k_H	$[\eta]$ (mL/g)	k_H
C45−5	71.8	0.39	53,1	0.54
C40−20	74.9	0.41	56.1	0.56
C28−22	64.2	0.37	47.8	0.55
C22−28	51.6	0.39	38.8	0.42
C15−35	48.0	0.38	35.5	0.46

The corresponding linear diblock copolymers of the sample C22−28 were prepared by the sequential addition to the initiator *sec*-BuLi, St (or St-d_8) and butadiene at room temperature. The polymerization of St-d_8 was left for completion for 24 h, and then a small amount of *sec*-BuOLi was added in a molar ratio of [*sec*-BuOLi]/[CLi] 4/1 (in order to have the same microstructure as the cyclics), followed by the addition of the appropriate amount of butadiene. The mixture was left for another 6 days, and the living chains were neutralized by using degassed MeOH. The molecular characteristics of the diblocks are given in Table 3.

Characterization of the Copolymers. SEC experiments were carried out at 25 °C using a Waters 610 pump, Waters model 410 differential refractometer, 996 diode-array UV detector and six columns with a continuous porosity range from 10^2 to 10^6 Å. THF was the carrier solvent. The number-average molecular weights (M_n) of the precursors and the final products were determined by using a Jupiter model 231 recording membrane osmometer (MO) at 37 °C. The solvent was toluene distilled over CaH_2. Nuclear magnetic resonance (NMR) spectra, recorded on a Bruker 300 MHz instrument with $CDCl_3$ as the solvent, at 25 °C, were used for the determination of the composition and the microstructure of PBd. In this case, due to the presence of *sec*-BuOLi, the 1,2-addition is slightly higher (13%) than the conventional (8%) one.

Viscometric data were analyzed using the Huggins equation:

$$\eta_{sp}/c = [\eta] + k_H[\eta]^2c + ... \quad (1)$$

and the Kraemer equation

$$\ln\eta_r/c = [\eta] + k_K[\eta]^2c + ... \quad (2)$$

where η_r, η_{sp}, and $[\eta]$ are the relative, specific, and intrinsic viscosities, respectively, and k_H and k_K are the Huggins and Kraemer constants, respectively. Virtually identical intrinsic viscosities were obtained by the two methods. All the measurements were carried out at 30 °C in toluene using Cannon-Ubbelohde dilution viscometers with a Schott-Geräte AVS 410 automatic flow timer. The viscometry results are shown in Table 4.

Characterization of the Micelles. Solution Preparation in Selective Solvents. Analytical grade *n*-decane was refluxed for 24 h over CaH_2 and fractionally distilled just before used. DMF was dried with NaOH for 24 h and refluxed over $MgSO_4$ for another 24 h under nitrogen atmosphere. Stock solutions were prepared by dissolving a weighted amount of sample in the appropriate volume of the solvent with occasional stirring. All samples were dissolved after 24 h at 60 °C. No polymer precipitation was observed from these solutions after standing at room temperature for several weeks. Before dynamic light scattering experiments, the solutions were

Table 5. Scattering Length Densities (ρ_i) of Polymeric Blocks and Solvents

polymeric chain or solvent	$\rho_i \times 10^{-10}$ (cm^{-2})
PBd	0.420
PS-d$_8$	6.36
protonated *n*-decane	−0.489
deuterated *n*-decane	6.58
protonated DMF	0.698
deuterated DMF	6.37

filtered through 0.45 μm nylon filters. Deuterated solvents were used as purchased from Aldrich, without further purification. In each case, a 1% (w/w) stock solution was prepared and diluted to the appropriate concentration.

Small-Angle Neutron Scattering Experiments. If the interparticle scattering contributions are neglected, the coherent macroscopic scattering cross section of a SANS experiment $(d\Sigma/d\Omega)(Q)$ is given by

$$\frac{d\Sigma}{d\Omega}(Q) = \frac{N_Z}{V}\langle|A(Q)|^2\rangle \tag{3}$$

where N_Z denotes the number of scatterers, V is a reference volume and $A(Q)$ the intraparticle scattering amplitude. The scattering vector Q is given by $4\pi\sin(\theta/2)/\lambda$, where θ is the scattering angle and λ the neutron wavelength.

For a particle consisting of a core and a shell, the scattering amplitude $A_{C,Sh}(Q)$ can be written as follows:

$$A_{C,Sh}(Q) = V_M(\rho_{Sh} - \rho_S)A_M(Q) + V_C(\rho_C - \rho_{Sh})A_C(Q) \tag{4}$$

Here ρ_C, ρ_{Sh}, and ρ_S are the scattering length densities of the core (C), shell (Sh) and the solvent (S), respectively. The scattering length density of a component i can be calculated by the following equation:

$$\rho_i = \frac{\sum b_z}{v_i} \tag{5}$$

where b_z is the coherent scattering length density of the atom z and v_i the respective volumes. V_M, V_C, $A_M(Q)$, and $A_C(Q)$ denote the volumes of the overall micelle the core, and the corresponding scattering amplitudes. The scattering length densities of the polymeric blocks and the solvents used are given in Table 5. In the case $\rho_{Sh} = \rho_S$ or $\rho_C = \rho_S$, then eq 4 is transformed into

$$A_{C,Sh}(Q) = V_C(\rho_C - \rho_{Sh})A_C(Q) \tag{6}$$

or

$$A_{C,Sh}(Q) = (\rho_C - \rho_{Sh})(A_C(Q)V_C - A_M(Q)V_M) \tag{7}$$

The first situation (eq 6) will be referred as core contrast whereas the second (eq 7) is referred to as shell contrast.

When *n*-decane was used as a selective solvent, two different contrasts were used, the core and the shell contrasts, by using solvent mixtures of deuterated and protonated *n*-decane. This was possible since the coherent scattering length density of PBd and PS-d_8 is between the protonated and deuterated *n*-decane (Table 5). The scattering length density of a mixture of protonated and deuterated solvent follows, with sufficient accuracy, a simple additivity rule:

$$\frac{\sum b_M}{v} = x\frac{\sum b_D}{v} + (1 - x)\frac{\sum b_H}{v} \tag{8}$$

where x is the volume fraction of the deuterated *n*-decane. Thus, core contrast ($\rho_M = \rho_s$) is obtained with $x = 0.129$ and shell contrast with $x = 0.97$ of deuterated *n*-decane. Three different concentrations, approximately 0.25, 0.50, and 1.0% (w/v) were measured for each copolymer at each contrast. To avoid backscattering, under shell contrast, 2 mm quartz cells were used (transmissions: 70−80%), whereas, under core contrast, 1 mm quartz cells were used (transmissions: 45 and 55%).

When DMF was the selective solvent, it was possible to match exactly the shell of the micelles, since deuterated DMF has practically the same scattering length density with PS-d_8. On the contrary, it was impossible to match exactly the core (PBd) of the micelles, since the $\sum b_i/v_i$ of PBd is much lower than the one of protonated DMF (Table 5). To ensure that the fits of the data under shell contrast are correct, one additional contrast was measured. As a consequence, three different contrasts were used, one in 100% (v/v) protonated DMF, one in 100% (v/v) DMF-d_7 (deuterated DMF), and one with 50/50% (v/v) protonated/deuterated DMF. One concentration was measured for each contrast approximately 0.50% (w/v), since it was found that in *n*-decane no structure factor was developed even at 1.0% (w/v) concentration.

In the case of samples with 100% (v/v) deuterated DMF and in the 50/50% (v/v) mixture of solvents, 2 mm quartz cells were used, whereas solutions with 100% (v/v) protonated solvent 1 mm quartz cells were used. The transmissions were between 75 and 85% in the first case, 55−65% in the second, and 45−55% in the third case.

All SANS experiments were performed at 25 °C, on the KWSII instrument at the research reactor FRJ2 at the Forschungszentrum Jülich GmbH. Three sample detector distances were used: 2, 8, and 18 m. For all detector distances, the neutron wavelength was 6.3 Å. Thus, a range of scattering vector of 2×10^{-3}Å$^{-1} \leq Q \leq 1.0 \times 10^{-1}$Å^{-1} was covered. The wavelength spread was $\Delta\lambda/\lambda = 18\%$. The raw data were corrected for background by subtracting the scattering of empty cell. These data were then corrected for different detector cell efficiency and calibrated to absolute units by a Lupolene secondary standard according to[29]

$$\frac{d\Sigma^S}{d(\Omega)}(Q) = \frac{T^L D^L (d\Sigma^L/d\Omega)A^L(R^S)^2}{T^S D^S I^L A^S (R^L)^2}(I^S - T^S B^S) \tag{9}$$

Here L and S refer to the Lupolene standard and sample, and D and T stand for thickness and transmission, respectively. A is the illuminated sample area, and R is the sample to detector distance. I is the intensity, and B is the experimental background. The value $T^L D^L(d\Sigma^L/d\Omega)$ for the Lupolene standard has been calibrated with vanadium to be $(7.34 \pm 0.03) \times 10^{-2}$.

Dynamic Light Scattering. DLS experiments were carried out at 25 °C on a series 4700 Malvern system composed of a PCS5101 goniometer with a PCS7 stepper motor controller, a Cryonics variable power Ar^+ laser, operating at 488 nm and with (10 mW) power, a PCS8 temperature control unit, and a RP98 pump/filtering unit. A 192-channel correlator was used for accumulation of the data. Correlation functions were analyzed by the cumulant method and the Contin software, provided by the manufacturer. The correlation function was collected at angles between 45 and 135°. There was no indication of the presence of unimers from Contin analysis at the concentration range studied for each sample (0.1−1.5% w/v). In this region the equilibrium is shifted in favor of micelles and the properties measured corresponds to those of the micelles. The solutions for SANS measurements were within the same concentration range. The ratio μ_2/Γ, where μ_2 is the second cumulant and Γ the decay rate was <0.1 for all concentrations and angles, indicating the low polydispersity of the micelles. Apparent diffusion coefficients at zero concentration were obtained by using the following equation:

$$D_{app} = D_{o,app}(1 + k_D c) \tag{10}$$

where D_{app} is the diffusion coefficient measured at each concentration and k_D the coefficient that gives the dependence of the diffusion coefficient with concentration. Apparent hydrodynamic radii, R_h were determined by eq 11, where k_B is the Boltzmann constant, T the absolute temperature and η_0

the viscosity of the solvent.

$$R_h = \frac{k_B T}{6\pi\eta_o D_{o,app}} \quad (11)$$

3. Results and Discussion

Synthesis and Characterization of Cyclic and Linear Block Copolymers. *s*-BuOLi was used as an additive in order to reduce the propagation rate of the polymerization of butadiene and to produce PBd with low polydispersity, as was shown in a previous paper.[30] The polymerization started from Bd and continued with styrene and not vice versa because the polymerization of styrene by DLI requires the presence of a strong promoter such as THF, which influences the microstructure of the PBd block. Finally the transformation of the styrenic to the dienic anion is necessary in order to facilitate the linking reaction (less steric hindrance).

Ma[31] has used a similar approach for the synthesis of cyclic PS-*b*-PBd copolymers. In this synthetic route, the cyclization was performed by adding dropwise a linking agent solution to the diluted α,ω-difunctional living triblock copolymer. Two different linking agents were used, either dichlorodimethylsilane or PEB. By Ma's way the linking agent is always added in an excess of living chains, increasing the probability of forming coupling products and as a consequence, lowering the yield of cyclization.

In our work, high dilution of the two reagents was always maintained. The total volume of the solvent was 1.8 L, keeping the concentration of the living chain ends in a concentration range of about 3×10^{-5} mol/L. This value is lower than the equilibrium concentration, $C_{eq} = (^3/_2\pi\langle r^2\rangle)^{3/2} M/N_A$,[2,32] which is the concentration in which the probability of intra- and intermolecular reaction is equal ($\sim 10^{-4}$ mol/L). $\langle r^2\rangle$ is the mean square end-to-end distance of the chain, M is the corresponding molecular weight and N_A is the Avogadro number. For the triblock copolymers, the sum of the end-to-end distance of the three separate blocks was used.

The "actual" concentration of the reagents was always kept lower than C_{eq}, provided that stoichiometric amounts are always added, and the reaction is complete within the time intervals of each step.

To ensure complete reaction within the time of each addition, BDSCE (the two chlorine atoms on two different Si atoms) was used as the linking agent. It is well established that two Si−Cl groups of each BDCSE molecule react very quickly with C−Li anions and present almost the same reactivity, even if one is reacted with a living polymeric chain.[33] As a consequence, the Si−Cl group that remains after the reaction of a difunctional living chain with one molecule of difunctional linking agent exhibits reactivity similar to that of the Si−Cl group of a free linking agent. Therefore, the probability of cyclization compared to the reaction of both functional groups of the polymeric chain with two different molecules of linking agent is equal. If Me_2SiCl_2 (the two chlorine atoms on the same Si) was used as linking agent, the Si−Cl group attached to a polymeric chain, for steric hindrance reasons, reacts slower than that of the free linking agent, and therefore more time is required between the addition of the two reagents.[34]

Approximately 5 g of the triblock precursor was used for cyclization. The overall yields of the cyclic copolymers were 30−40%. The cyclization reaction was performed in benzene which is a very good solvent for both blocks, PS and PBd. As a consequence, the copolymer chains are swollen during the cyclization and the minimum amount of permanent knots are expected to be formed. The polydispersity index of the cyclics was equal within experimental error to that of the corresponding linear precursors.

One indication of the formation of cyclic copolymers is the lower molecular weight obtained by SEC compared to the linear precursors. The ratio of $M_{pC}/M_{pT} = 0.73-0.75$ in all five copolymers, where M_{pC} and M_{pT} are the peak molecular weights of the cyclic and triblock, respectively. This is in good agreement with the values found by Leppoittevin et al.[7] for ring PS homopolymers. In that work, the purification of the cyclic copolymers was performed by using preparative liquid chromatographic separation, and information for the chemical structure was obtained by using matrix-assisted laser desorption/ionization time-of-flight mass spectrometry (MALDI−TOF). The formation of the cyclic copolymers is also supported by the presence of a peak at 0.3 ppm in the ^{1}H NMR spectrum, which is attributed to the 12 protons of the four $-CH_3$ groups of the linking agent attached to the cyclic copolymer.

In our case, the formation of the cyclic structure is also supported by $g' = [\eta]_c/[\eta]_l$, where $[\eta]_c$ and $[\eta]_l$ are the intrinsic viscosity of the cyclic and the corresponding linear precursor before the cyclization (Table 3). g' values between 0.73 and 0.75 were obtained. This ratio is higher than the values of 0.66−0.68 found by Roovers et al.[2] and Leppoittevin et al.[7] However, an expansion to the dimensions of a cyclic copolymer is expected since an increased number of heterocontacts is expected to be present between incompatible polymeric blocks. Iatrou et al.[35] found a similar influence of the heterocontacts on the dimensions of 3-miktoarm stars of the A_2B type in dilute solution. In that work, a higher intrinsic viscosity was found for the miktoarm stars compared to the intrinsic viscosity of the corresponding star homopolymers. Ma,[31] for a copolymer with similar molecular characteristics, found a value of 0.79. The k_H constants of the cyclics were significantly higher which indicates that the interactions between the polymeric chains are increased compared to the ones of the triblock copolymer precursor. Since there are not other results concerning the g' and k_H values of a diblock cyclic copolymer, it cannot be used as a reliable parameter for the evaluation of their purity.

Characterization of the Micelles. The linear triblock and the corresponding cyclic copolymers C22−28, D22−28, and (D22−28)/2 (Tables 1 and 2) constitute a series with similar molecular characteristics (composition and total molecular weights, except (D22−28)/2, which has half the molecular weight of the others. This will be referred as half-diblock). To investigate the purity of the cyclics and the influence of the macromolecular architecture to the micellar behavior, the molecular characteristics of the micelles were obtained by SANS and DLS. In *n*-decane, the collapsed PS-d_8 chains form the core and the dissolved PBd chains are in the shell of the micelle that keep the aggregate in solution, whereas in DMF the situation is reversed (Scheme 3).

SANS Measurements in *n*-Decane. The coherent macroscopic scattering cross sections ($d\Sigma/d\Omega$) for the cyclic copolymer C22−28, the linear precursor, and the corresponding diblocks with the same and half the

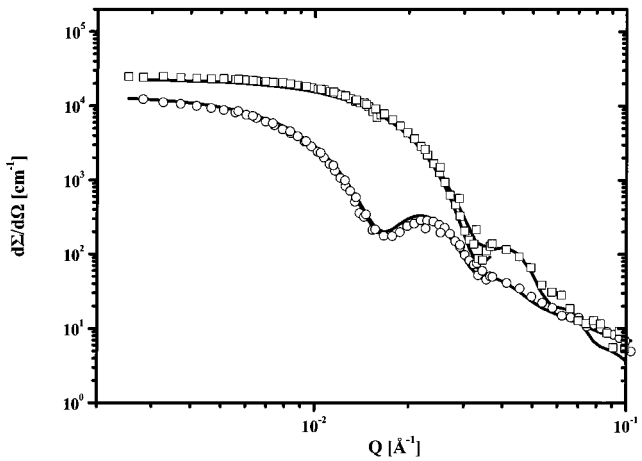

Figure 2. Scattering cross section dΣ/dΩ vs Q under core (□) and shell (○) contrasts of the cyclic copolymer C22−28 in *n*-decane at 25 °C and concentration 0.50% (w/v). The solid line represents the calculated cross sections, and the dots represent the experimental data.

Scheme 3

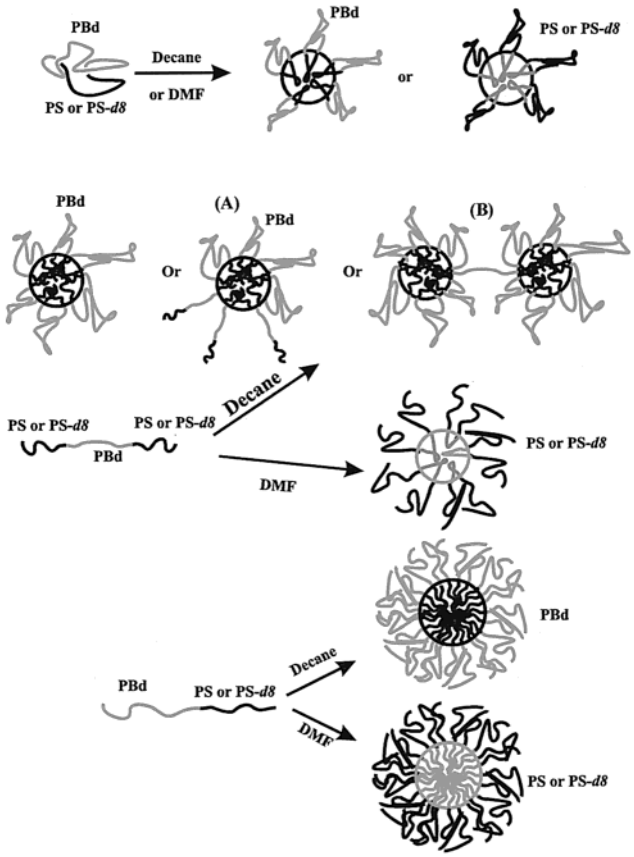

molecular weights in both contrasts (core and shell) in *n*-decane and 0.5% (w/v) concentration, evaluated according to eqs 3−9, are shown in Figures 2−5.

The curve exhibits a well-pronounced secondary maximum and in some cases a weak third maximum. This implies that the aggregates formed are relatively uniform in size, and present well-defined structure. Moreover, the sharpness of the minima under core and shell contrasts indicates a high symmetry of the aggregates.

To find the form of the micelles, model fitting was performed. It was found that a spherical core/shell structure could fit very well the experimental data.

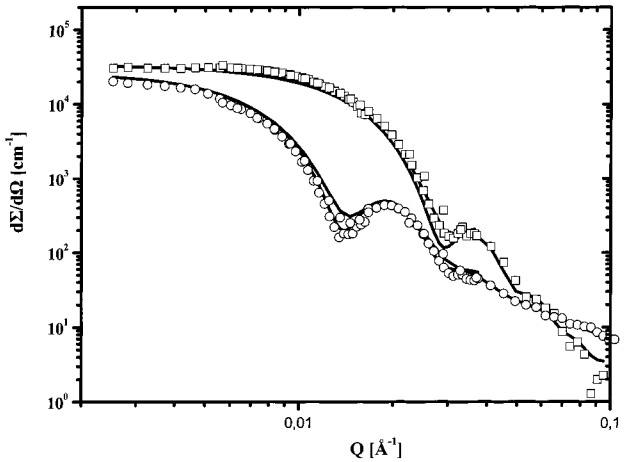

Figure 3. Scattering cross section dΣ/dΩ vs Q under core (□) and shell (○) contrasts of the triblock copolymer C22−28 in *n*-decane at 25 °C and concentration 0.50% (w/v). The solid line represents the calculated cross sections, and the dots represent the experimental data.

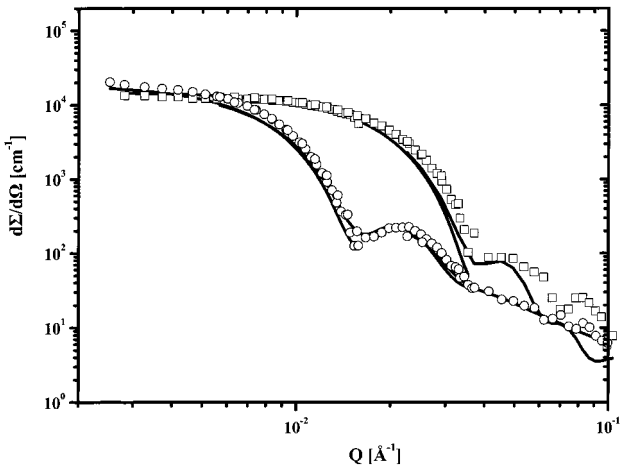

Figure 4. Scattering cross section dΣ/dΩ vs Q under core (□) and shell (○) contrasts of the diblock copolymer D22−28 in *n*-decane at 25 °C and concentration 0.50% (w/v). The solid line represents the calculated cross sections, and the dots represent represent the experimental data.

Therefore, the scattering amplitude introduced in eq 4 for this model are given by[36]

$$A_{M,C}(Q) = \frac{3(\sin(Qr_1) - Qr_1\cos(Qr_1))}{(Qr_1)^3} \qquad (12)$$

where r_1 is either the core or the outer periphery of the micelle. To obtain a comparison on an absolute intensity scale, the model used required the concentration of the polymers, the molecular weight of each arm of the blocks (in case they were split in two arms the total molecular weight was introduced) measured by MO, the density of the polymeric chain of the core and shell, and the scattering length densities of the polymeric chain of the core, shell, and solvent as a fixed input. To perform a convolution to account for the instrumental resolution in addition the neutron wavelength λ, the dimensions of sample cell, the collimation length, the detector distance, and the wavelength spreading, $\Delta\lambda/\lambda$, were used to model the resolution function; i.e., the calculated scattering cross sections were convoluted by a Gaussian type resolution function taking into account the experimental parameters, according to Pedersen et al.[37]

Table 6. Molecular Characteristics of the Micelles in *n*-Decane at 25 °C of the C22−28 Cyclic Copolymers, the Corresponding Linear Precursor and the Diblock Copolymers

sample	M_n(PBd) $\times 10^{-3}$	M_n(PS-d_8) $\times 10^{-3}$	P	R_c (nm)	R_o(SANS) (nm)	f_{star}	σ_C (nm)	σ_{Sh} (nm)	R_h(DLS) (nm)	k_d
diblock	21.0	23.2	280	13.2	28.3	1	2	2.1	28.4	5.7
(diblock)/2	12.0	14.0	220	10.0	19.6	1	1	1.7	20.5	3.7
triblock	23.0	30.0	400	17.2	28.0	0.37	3	2.7	31.6	∼0
cyclic	23.0	30.0	210	14.5	24.0	0	2	1.7	26.8	−6.2

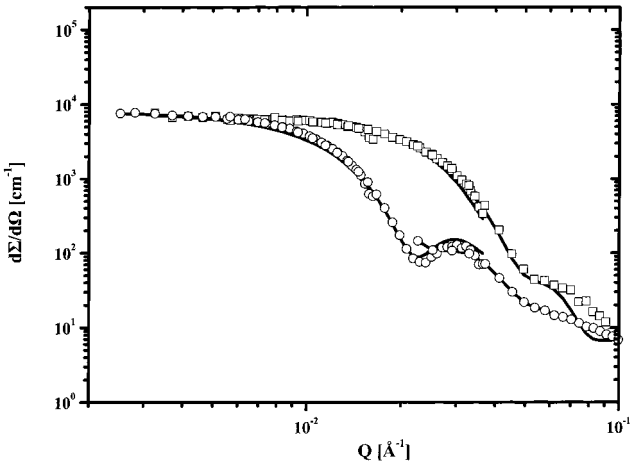

Figure 5. Scattering cross section dΣ/dΩ vs Q under core (□) and shell (○) contrasts of the diblock copolymer (D22−28)/2 in *n*-decane at 25 °C and concentration 0.50% (w/v). The solid line represents the calculated cross sections, and the dots represent the experimental data.

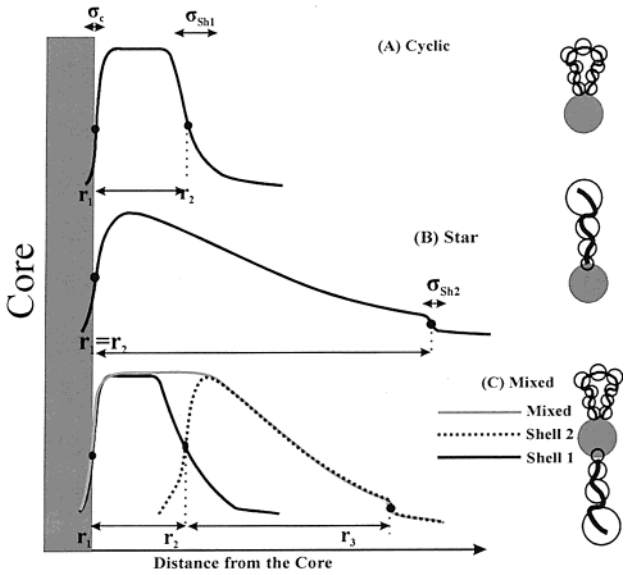

Figure 6. Volume fraction of the coronal bulk polymer as a function of the distance of the surface of the core: (A) constant density profile (cyclics in both solvents); (B) starlike density profile (diblocks and triblock in DMF); (C) mixed density profile (triblock in *n*-decane).

Instead of an idealized sphere form factor (eq 12), a smeared out density profile ($\varphi_c(r)$) for the micelle core was used

$$\varphi_c(r) = \varphi_c^0 \frac{1}{1 + \exp\frac{r - r_1}{\sigma_C}} \tag{13}$$

where φ_c^o is the density of the PS-d_8 in the core and σ_C is a fit parameter for the width of the core boundary, due to its roughness or/and deformation from the spherical shape. The Fourier transform of the density profile $\varphi_c(r)$ replaces the scattering amplitude of eq 12. Only in the limit of an infinite thin smearing ($\sigma_c \rightarrow 0$) is eq 12 retained.

First, the scattering curve under core contrast was fitted independently using eq 4. Thus, the core radius was calculated by using

$$R_C = \left(\frac{3PM_C}{4\pi\rho_C N_A}\right)^{1/3} \tag{14}$$

where M_C is the total molecular weight of the PS-d_8 blocks, $\rho_C = 1.12$ g/mL, the density of PS-d_8, and N_A is the Avogadro number. The only adjustable parameters were the aggregation number P and σ_C (note that R_c and r_1 are identical here). The obtained values are given in Table 6. The very small smearing indicates a low polydispersity or/and low interface roughness of the core.

The model used for the fit (Figure 6) under shell contrast had the option of splitting the bulk volume of the shell polymer in two parts, shell 1 close to the core with constant density profile and radius r_2 (case a), and shell 2, in the outer periphery with a density profile of a star polymer and radius r_3 (case b). For that purpose, a parameter f_{star} was introduced, which is the fraction of the bulk volume $V_{Sh,tot}$ of the shell 2. In this case f_{star} describes the relative polymer amounts in the shells (case c). A detailed description of the fitting functions is given in the Appendix. The aggregation number and therefore the bulk volume of the shell polymer were calculated from the fit of the data under core contrast. The scattering length density of the mixture of polymer and solvent was the average, calculated from the volumes of the bulk polymer and solvent.

The density of PBd used was 0.91 g/mL. The fit parameters under shell contrast were f_{star}, σ_i and d_i. A simultaneous fit under core and shell contrast was always performed. P, f_{star}, σ_i, R_C, and R_o of the micelles obtained are given in Table 6. Here we set $R_o = r_3$ identical.

From Table 6, the f_{star} value of 1, obtained in the case of the two diblock copolymers, indicates that a starlike density profile can fit very successfully the experimental data of the shell. This density profile follows the $r^{-4/3}$ expansion of the PBd polymeric chains presented by Daoud and Cotton[38] for the density profile of a starlike molecule. The low values of σ verify the already indicated low polydispersity of the micelles and their spherical form.

In the case of triblock copolymer, interchain micellization is possible, since *n*-decane is a poor solvent for PS-d_8 end blocks. However, no indication of the formation of such aggregates was found, since no indication of a modulation at low Q due to a structure factor was observed in the experimental data under core or shell contrast. The data were fitted by a simple form factor of a sphere. An aggregation number of 400 was found

for the triblock copolymer, which is much higher than the one of the corresponding diblock. A mixed shell density profile composed of a 63% constant and 37% starlike density profile ($f_{star} = 0.37$) was necessary to be used in order to fit the data. This indicates that the micelles contain some triblock copolymers with the form of dangling chains (Scheme 3). The PS-d_8 blocks which are in the outer periphery are collapsed, and therefore they are very small in volume and randomly distributed. As a consequence, they do not contribute significantly in the overall scattering under core contrast. In the case of 37% of the PS-d_8 dangling chains, only half of the amount of PS-d_8 contributes to the formation of the core and therefore the actual aggregation number is 520. The increased σ value of 27 Å found in the case of the triblock copolymers is higher that the corresponding values of the diblock and cyclic copolymers. This indicates an increased roughness of the outer periphery or/and slight deviations from the spherical form. The density profile of the micelles is shown in Figure 6. The formation of spherical noninterconnected micelles has been observed in similar systems, by Tanaka et al.[39] and Balsara et al.[22] for copolymers with composition close to 50%. However, in these works, a lower aggregation number was found, compared to the one of the linear diblock analogues.

Surprisingly, in the case of cyclic copolymer the data were better fitted when a 100% ($f_{star} = 0$) constant density profile was used. The constant density profile can be explained by the formation of loops of the PBd chains. Since there is no free chain end, all monomeric units are almost equivalent, having the same excluded volume, and cannot expand with an $r^{-4/3}$ dependence of the density profile of a starlike molecule[38] (Figure 6). The corresponding σ value for the cyclic is much lower, supporting the conclusion that the micelles are nearly monodisperse.

The aggregation numbers obtained from the fits are on the order of

$$P_T > P_D > P_{D/2} > P_C \quad (15)$$

where P_T, P_D, $P_{D/2}$, and P_C are the aggregation numbers of the triblock, diblock, half-diblock, and cyclic copolymers, respectively.

A lower aggregation number of the half-diblock compared to the diblock copolymer was expected since the aggregation number strongly depends on the molecular weight of the collapsed chain. Moreover, a lower aggregation number of the cyclic copolymer was expected compared to the one of the corresponding linear diblock copolymer, due to the necessity of the formation of loops of the dissolved chains, which decreases the possible conformations and therefore introduces an entropic penalty. More quantitative analysis on the aggregation numbers of several architectures will be discussed below on the basis of scaling models.

The geometrical characteristics of the micelles are shown in Table 7. In this table, the coronal thickness $H = R_o - R_C$ along with the core area per junction point A_C is calculated. The coronal thickness can be compared with the end-to-end distance of a polymeric chain in a Θ solvent. The core area per junction point A_C was calculated by using the following equation:

$$A_C = \frac{4\pi R_C^2}{P} \quad (16)$$

Table 7. Geometrical Characteristics of the Micelles of the C22−28 Cyclic Copolymers, the Corresponding Linear Precursor, and the Diblock Copolymers in *n*-Decane and DMF at 25 °C

	n-decane			DMF		
sample	R_c (nm)	H_{corona} (nm)[a]	A_c (nm^2)	R_c (nm)	H_{corona} (nm)[a]	A_c (nm^2)
diblock	13.2	15.1	7.8	21.3	7.5	5.4
diblock/2	10.0	9.6	12.6	14.3	5.0	4.3
triblock	17.2	10.8	8.8	19.0	5.9	3.2
cyclic	14.5	9.5	12.6	16.5	5.1	3.8

[a] $H_{corona} = R_o - R_c$.

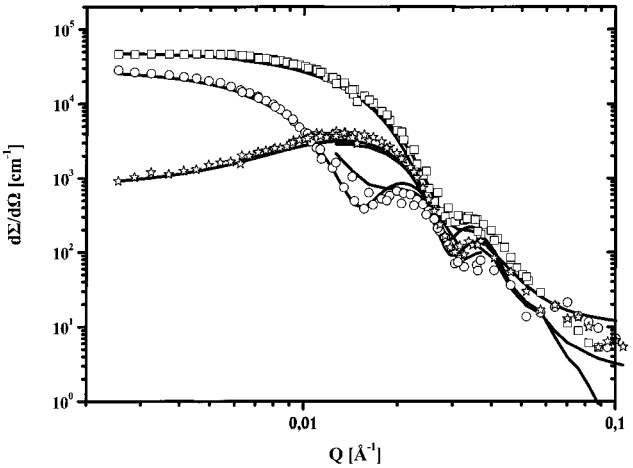

Figure 7. Scattering cross section dΣ/dΩ vs Q under core (□), intermediate (☆), and shell (○) contrasts of the cyclic copolymer C22−28 in DMF at 25 °C and concentration 0.50% (w/v). The solid line represents the calculated cross sections, and the dots represent the experimental data.

In the case of cyclic and triblock copolymers, the calculated area has been divided by two, since there are two junction points per PBd chain. It can be seen that the coronal thickness of the cyclic and half-diblock are equal, while the one of the triblock is slightly larger and the one of the diblock the largest. This order is expected since the mean square radius of gyration of a ring polymer of length N is identical to the mean square radius of gyration of a linear chain with length $N/2$.[40,41] These numbers are comparable since the areas per junction point, and therefore the stretchings of the polymeric chains due to crowding effects, are identical. The higher shell thickness of the triblock copolymer maybe due to the presence of the dangling chains. It is well-known that the ratio of mean square radius of gyration between a cyclic and linear chain is equal to 0.5. On the basis of this, the ratio of the shell thickness between the linear diblock and the cyclic copolymer should be equal to the square root of 0.5, i.e., 0.7. The ratio was found equal to 0.63, and the difference may be due to the smaller area per junction point of the linear diblock copolymer which shows that the PBd chains are more stretched and therefore more elongated.

SANS Measurements in DMF. The coherent macroscopic scattering cross sections (dΣ/dΩ) for the copolymers in DMF evaluated according to eqs 3−9 are shown in Figures 7−10.

The relatively sharp secondary maximum and in some cases a weak third maximum implies that the aggregates formed are relatively uniform in size and symmetric. The form of the scattering cross sections obtained under core contrast in this solvent is similar

Table 8. Molecular Characteristics of the Micelles in DMF at 25 °C of the C22−28 Cyclic Copolymers, the Corresponding Linear Precursor, and the Diblock Copolymers

sample	M_n(PBd) $\times 10^{-3}$	M_n(PS-d_8) $\times 10^{-3}$	P	R_c (nm)	R_o(SANS) (nm)	f_{star}	σ_C (nm)	σ_{Sh} (nm)	R_h(DLS) (nm)	k_d
diblock	21.0	23.0	1050	21.3	28.8	1	2	2.1	30.1	6.6
diblock/2	12.0	14.0	585	14.3	19.3	1	2	2.0	19.9	4.8
triblock	23.0	30.0	680	19.0	24.9	1	3	2.5	26.4	6.1
cyclic	23.0	30.0	450	16.5	21.4	0	2	2.3	23.2	5.2

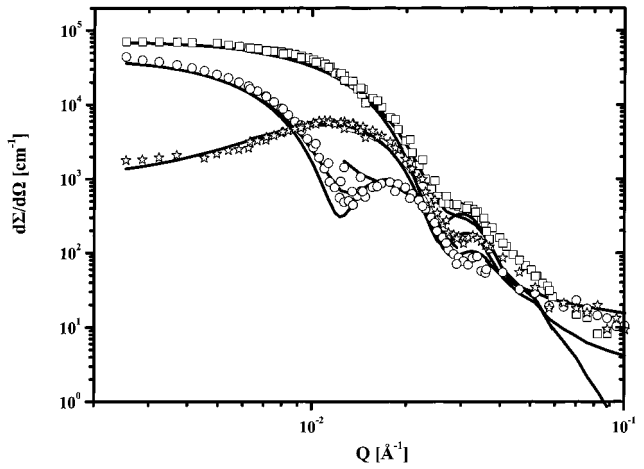

Figure 8. Scattering cross section dΣ/dΩ vs Q under core (□), intermediate (☆), and shell (○) contrasts of the triblock copolymer C22−28 in DMF at 25 °C and concentration 0.50% (w/v). The solid line represents the calculated cross sections, and the dots represent the experimental data.

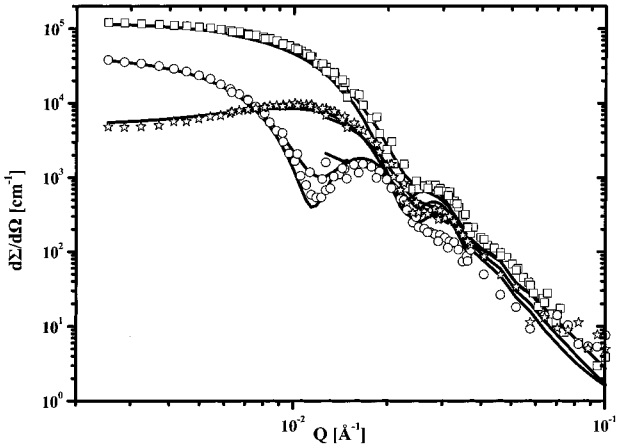

Figure 9. Scattering cross section dΣ/dΩ vs Q under core (□), intermediate (☆), and shell (○) contrasts of the diblock copolymer D22−28 in DMF at 25 °C and concentration 0.50% (w/v). The solid line represents the calculated cross sections, and the dots represent the experimental data.

to the one obtained in *n*-decane. As a consequence, a model of a spherical core/shell structure was used in order to fit the data.

The same fit model described above was used. The molecular characteristics of the micelles formed in this case are shown in Table 8.

In this case, a constant density profile was used to fit the data only of the cyclic copolymer, whereas a starlike density profile could fit the experimental data of the triblock, and two diblock copolymers.

The aggregation numbers obtained in DMF are of the order

$$P_D > P_T > P_{D/2} > P_C \qquad (17)$$

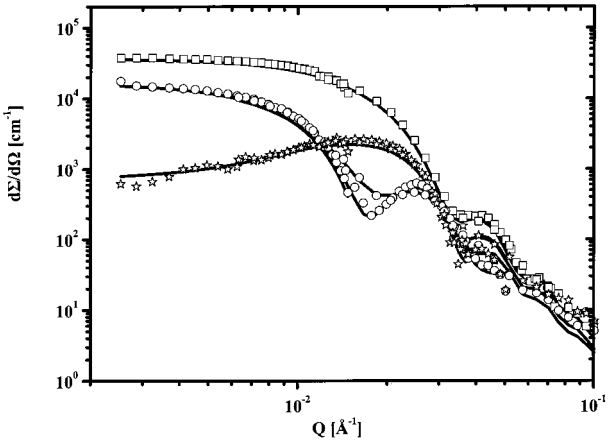

Figure 10. Scattering cross section dΣ/dΩ vs Q under core (□), intermediate (☆) and shell (○) contrasts of the diblock copolymer (D22−28)/2 in DMF at 25 °C and concentration 0.50% (w/v). The solid line represents the calculated cross sections, and the dots represent the experimental data.

The aggregation number of the half-diblock was expected to be lower than that of the diblock like in *n*-decane. The aggregation number of the triblock is expected to be lower than the one of the corresponding diblock due to the entropic penalty of the looped PBd chains in the core and the crowding of the PBd chains in the shell. Finally the aggregation number of the cyclic should be lower than the corresponding triblock due the additional entropic penalty from the PBd loops in the corona. More quantitative analysis concerning the aggregation numbers will be made below.

The geometrical characteristics of the micelles are shown in Table 7. The same order in coronal thickness, H, was found like in the case of the micelles in *n*-decane. The lower ratio (0.6) of the coronal thickness between the diblock and cyclic copolymer maybe due to the much lower area per junction point of the diblock copolymer which would oblige the PS-d_8 chains to become stretched and, as a consequence, would increase the dimensions of the PS-d_8 coronal chains.

Dynamic Light Scattering. The R_h values of the micelles formed in both solvents along with the k_D values obtained by DLS are shown in Tables 6 and 8. The obtained values are 5−10% larger than the one obtained from SANS. For hard spheres, the static and dynamic radii should be identical. The difference may be due to experimental uncertainty or to the fuzziness of the outer periphery of the micelle.

Surprisingly, the value of k_D of the triblock in *n*-decane was almost zero, while the corresponding value of the cyclic was negative. k_D is composed of thermodynamic as well as frictional components. For a dilute solution of homopolymers, k_D can be expressed as

$$k_D = 2A_2M_w - k_f \qquad (18)$$

where A_2 is the second virial coefficient that depends on intermolecular interactions, M_w is the weight-aver-

age molecular weight of the polymer, and k_f is related to the frictional drag that opposes the motion of the molecules.[42] Since the friction coefficient for similar polymer solutions is related to their concentration, their values are expected to be similar for the four different copolymers with three different architectures, because they were measured in similar concentrations. As a consequence, the lower k_D values may be due to the lower A_2 values in the case of cyclics, compared to the one of the triblock and the diblocks. Similar results were obtained in DMF (Table 7).

4. Interpretation in Terms of Scaling Models

The free energy F of a single chain incorporated in a micelle far away from the critical micelle concentration is approximated as a sum of three contributions:

$$F = F_{int} + F_{Sh} + F_C \tag{19}$$

The first term F_{int} denotes the interfacial contribution to the free energy associated with the core−corona interface given by

$$F_{int} = \frac{4pR_C^2\gamma}{P_{eq}} \tag{20}$$

where γ denotes the interfacial tension between the solvent and the collapsed chains, and P_{eq} is the equilibrium aggregation number. The contributions F_C and F_{Sh} are related to chain stretching in the core and the shell, respectively. Iatrou et al.[24] found that a scaling model of an intermediate regime, i.e., micelles with $H \leq R_C$, where $H = R_o - R_C$, could describe the experimental results of the linear diblock PS−PI in *n*-heptane or *n*-decane along with the $(PI)_3PS\text{-}d_8(PI)_3$ super-H block copolymers. In that work the aggregation number of the super-H block copolymers stars were found to be 1 order of magnitude lower than the corresponding linear diblocks. It was found that the intermediate regime occurs when

$$N_{PI}^{15/11} f^{2/5} \ll N_{PS} \ll N_{PI}^{18/11} f^{7/6} \tag{21}$$

where f is the number of PI chains per PS chain of the super-H copolymers, and $N_{PS,PI}$ the number of monomeric units of PS or PI. In the case of diblocks, f equals 1. Although this model is valid for comparison of the aggregation numbers between copolymers with different architectures, the values calculated are much lower than the experimental ones.

Nagarejan and Ganesh[23] developed a more comprehensive model which relates the core radius and coronal thickness H of micelles of AB diblock copolymers in selective solvents. Six different contributions to the micellar free energy are considered in this model. The reference state for the calculation of the energy is a single block copolymer in the selective solvent. Each free energy of the core and shell consists of two terms. The first term includes entropy contributions when passing from the reference to micellar state. The second term includes contributions due to chain deformation. The interfacial free energy is equal to the one given in eq 20. In this model, the equilibrium micelle is obtained from the minimization of the free energy per molecule with respect to the independent variables of core and outer radius. By comparison of the experimental data from three different copolymer/solvent systems and numerical results from the theory, the following scaling relation was established:

Table 9. Calculated Aggregation Numbers in *n*-Decane and DMF

	n-decane		DMF	
sample	P_{exp}[a]	P_{calc}[b]	P_{exp}[a]	P_{calc}[b]
cyclic	210		450	
triblock	360		680	506
diblock	280	324	1050	1070
diblock/2	220	216	585	686

[a] Experimentally found aggregation numbers. [b] Calculated aggregation numbers by the scaling models.

$$P_{eq} = \frac{4\pi m_C(\gamma l_S^2/k_BT) + (4\pi/3)m_C^{1/2} + (4\pi/3)m_{Sh}^{1/2}(R_C/H)}{1 + m_C^{-1/3} + (m_C/m_{Sh})(H/R_C)^2} \tag{22}$$

In this equation l_S denotes the characteristic length of a solvent molecule, which is calculated from its volume $l_S = v_S^{1/3}$, $m_{C,Sh}$ are the ratios of the volumes of the core or shell blocks and a solvent molecule: $m_{C,Sh} = v_{C,Sh}/v_S$.

For a comparison with our results, we used the radii from Tables 5 and 7, as obtained from the model fitting of SANS data. Concerning the results in *n*-decane, the models were applied only for the diblock copolymers, because the triblock copolymer is more complicated, the aggregation number cannot be calculated. The models will be applied in the results in DMF. With l_S of *n*-decane equal to 6.87 Å, m_C of the cyclic and triblock copolymers are equal to 132.9 for both, m_C for the diblock copolymer is equal to 116.1, and m_C for the half-diblock is equal to 62. The corresponding values in the same solvent for the shell are 123.5 for the cyclic, triblock, and diblock copolymers and 61.8 for the half-diblock copolymer. The l_S value for DMF is 5.04 Å, while m_C for the diblock, triblock, and cyclic copolymer is 313.8. The corresponding value for the half-diblock is 157. The m_{Sh} values are 337.5 for the triblock and cyclic copolymers, 294.7 for the diblock, and 157.4 for the half-diblock copolymer. An interfacial tension of $\gamma = 5.1$ dyn/cm between PS and *n*-decane was used,[43,23] whereas a value of $\gamma = 12.5$ dyn/cm was used for the PBd and DMF pair. The interfacial surface tension between DMF and PBd was measured from the contact angle between the two liquids. The aggregation numbers obtained are shown in Table 9.

To calculate the aggregation number of a triblock copolymer in DMF, where the middle part is collapsed, one has to take into account the entropic penalty that comes from the stretching of the PBd chain in the core in order to bring the junction points on the interface and the increased repulsive monomer−monomer interactions within the starlike corona, since the number of arms are doubled. Since the core is considered to be in the melt state, the PBd chains are already deformed in order to fill the space of the core. As a consequence, the entropic penalty of the deformation of PBd chains to bring the two junction points to the interface is much smaller than the repulsive interactions of the crowded monomers within the corona. This penalty has been calculated to reduce the aggregation number by a factor of $f^{-7/6}$,[24] where f is the number of chains in the corona per collapsed chain in the core (for triblocks $f = 2$). This reduces the calculated aggregation number to 506. This

is much lower than the experimentally found, because the term $f^{-7/6}$ was applied for the super-H miktoarm star copolymers, where the functionality was 6, and as a consequence is overestimated in the case of the triblocks.

To calculate the aggregation number of the cyclic copolymers, one has to take into account all the entropic and enthalpic penalties already mentioned for the triblock copolymers with a collapsed middle chain and, additionally, the reduction in entropy due to loop formation of the connected end blocks in the corona. Hadjiioannou and ten Brinke[44] calculated the free energy of the micelle, treating the looped block as two separate linear chains with half molecular weight. The contribution to the total free energy from the reduction in entropy, according to that work, is estimated to be

$$F_{\text{loop}} = \beta\left[\frac{3PkT}{2}\ln(N_{\text{A}})\right] \tag{23}$$

where β is a correction factor close to unity, N_{A} is the number of monomeric units of the dissolved chain, P is the aggregation number, and k is the Boltzmann constant. However, this equation does not relate the aggregation number of a cyclic polymer with the corresponding value of a linear diblock copolymer analogue.

Booth et al.[26] in a system of ethylene oxide and propylene oxide (PPO) block copolymers, found that triblock copolymer exhibited the lowest aggregation number, by comparing the micellar behavior of the cyclic copolymer and the linear diblock and triblock analogues. In their triblocks, the collapsed chain was the middle PPO block.

5. Conclusions

The synthesis and characterization of a series of model cyclic diblock copolymers has been presented. The characterization analysis by MO, UV and NMR spectroscopy, and viscometry indicated the formation of the cyclic architecture. However the degree of the purity could not be estimated by these methods. The micellar behavior of three different architectures showed that

a. By using BDCSE as a linking agent instead of dichlorodimethylsilane, the linking reaction is performed quicker, and it is possible to perform a controlled and multistep addition of this reagent, since is not volatile. These advantages increase the yield of the cyclization reaction.

b. The cyclic copolymers present the lowest aggregation number, compared to the corresponding values of a triblock and diblock copolymers with equal and half molecular weights. This is due to the entropic penalties from the looped architecture.

c. The shell thickness of the cyclic copolymer in both solvents is equal to the shell thickness of the diblock copolymer with the same composition but half the molecular weight. This was expected since the mean square radius of gyration of a ring polymer of length N, is expected to be identical with the mean square radius of gyration of a linear chain with length $N/2$.

d. The bulk density profile of the triblock copolymer in *n*-decane, where the end blocks are the collapsed part, can be described assuming there are dangling chains on the micelle. On the contrary, the cyclic copolymer could be represented assuming a constant density profile due to the looped corona that does not allow the PBd arm to expand like an arm of a star. On the basis of this difference, the purity of the cyclics is higher than 87%.

Acknowledgment. The authors would like to acknowledge the BMBF for financial support, Dr. J. Roovers and Dr. L. Willner for fruitful discussions, and Prof. Spyros Anastasiadis for the surface tension measurements.

Appendix

The equation for the density profile of the shell 1 (case a) is given by

$$\phi_{\text{sh1}} = \phi_{\text{sh1}}{}^{0}\left(1 - \frac{1}{1+\exp\dfrac{r-r_1}{\sigma_c}}\right)\left(\frac{1}{1+\exp\dfrac{r-r_2}{\sigma_{\text{sh1}}}}\right) \tag{A1}$$

The equation for the density profile of the shell 2 (case b) is given by

$$\phi_{\text{sh2}} = \phi_{\text{sh2}}{}^{0}\left(1 - \frac{1}{1+\exp\dfrac{r-r_2}{\sigma_{\text{sh1}}}}\right)\left(\frac{1}{1+\exp\dfrac{r-r_3}{\sigma_{\text{sh2}}}}\right)\frac{1}{r^{4/3}} \tag{A2}$$

The case c combines the two shells. Here the parameter f_{star} describes the relative amounts of shells 1 and 2 by the following definition:

$$f_{\text{star}} = \frac{\int \phi_{\text{sh2}}\,\mathrm{d}r}{\int \phi_{\text{sh1}}\,\mathrm{d}r + \int \phi_{\text{sh2}}\,\mathrm{d}r}$$

References and Notes

(1) Fiers, W.; Sinsheimer, R. L. *J. Mol. Biol.* **1962**, *5*, 424. Dulbecco, R; Vogt, M. *Proc. Natl. Acad. Sci., U.S.A.* **1963**, *50*, 236.
(2) Roovers, J.; Toporowski, P. *Macromolecules* **1983**, *16*, 843.
(3) Roovers, J.; Toporowski, P. *J. Polym. Sci., Part B: Polym. Phys.* **1988**, *26*, 1251.
(4) Ishizu, K.; Ichimura, A. *Polymer* **1998**, *25*, 6555.
(5) Cramail, S.; Schappacher, M.; Deffieux, A. *Macromol. Chem. Phys.* **2000**, *201*, 2328.
(6) Kubo, M.; Takeuchi, H.; Ohara, T.; Itoh, T.; Nagahata, R. *J. Polym. Sci., Part A: Polym. Chem.* **1999**, *37*, 2027.
(7) Leppoittevin, B.; Dourges, M.; Masure, M.; Hemery, P.; Baran, K.; Cramail, H. *Macromolecules* **2000**, *33*, 8218.
(8) Yin, R.; Hogen-Esch, T. E. *Macromolecules* **1993**, *26*, 6952.
(9) Mandani, A.; Favier, J.; Hemery, P.; Sigwalt, P. *Polym. Int.* **1992**, *27*, 353.
(10) Oike, H.; Hamada, M.; Eguchi, S.; Danda, Y.; Tezuka, Y. *Macromolecules* **2001**, *34*, 2776.
(11) Gan, Y.; Zöller, J.; Yin, R.; Hogen-Esch, T. *Macromol. Chem., Makromol. Symp.* **1994**, *77*, 93.
(12) Jo, W.; Jang, S. *J. Chem. Phys.* **1999**, *111*, 1712.
(13) Lee, H.; Lee, H.; Lee, W.; Chang, T.; Roovers, J. *Macromolecules* **2000**, *33*, 8119.
(14) Tuzar, Z.; Kratochvil, P. *Surf. Colloid Sci.* **1993**, *15*, 1.
(15) Stejskal, J.; Hlavata, D.; Sikora, A.; Konak, C.; Plestil, J.; Kratochvil, P. *Polymer* **1992**, *33*, 3675.
(16) Bahadur, P.; Sastry, N.; Marti, S.; Riess, G. *Colloids Surf.* **1985**, *16*, 337.
(17) Oranli, L.; Bahadur, P.; Riess, G. *Can. J. Chem.* **1985**, *63*, 2691.
(18) Antonnietti, M.; Heinz, S.; Schmidt, M.; Rosenauer, C. *Macromolecules* **1994**, *27*, 3276.
(19) Forster, S.; Zisenis, M.; Wenz, E.; Antonietti, M. *J. Chem. Phys.* **1996**, *104*, 9956.
(20) Calderara, F.; Riess, G. *Macromol. Chem. Phys.* **1996**, *197*, 2115.
(21) Antonietti, M.; Forster, S.; Oestestreich, S. *Macromol. Symp.* **1997**, *121*, 75.

(22) Balsara, N.; Tirrell, M.; Lodge, T. *Macromolecules* **1991**, *24*, 1975.
(23) Nagarajan, R.; Canesh, K. *J. Chem. Phys.* **1989**, *90*, 5843.
(24) Iatrou, H.; Willner, L.; Hadjichristidis, N.; Halperin, A.; Richter, D. *Macromolecules* **1996**, *29*, 589.
(25) Pispas, S.; Hadjichristidis, N.; Potemkin, I.; Khokhlov, A. *Macromolecules* **2000**, *33*, 1741.
(26) Booth, C.; Attwood, D. *Macromol. Rapid. Commun.* **2000**, *21*, 501.
(27) Hadjichristidis, N.; Iatrou, H.; Pispas, S.; Pitsikalis, M. *J. Polym. Sci. A: Polym Chem.* **2000**, *38*, 3211.
(28) Ignatz-Hoover, F. Ph.D. Thesis, University of Akron: 1989.
(29) Pyckout-Hintzen, W.; Springer, T.; Forster, F.; Gronski, W.; Frischkorn, C. *Macromolecules* **1991**, *24*, 1269.
(30) Iatrou, H.; Mays, J.; Hadjichristidis, N. *Macromolecules* **1998**, *31*, 6697.
(31) Ma, J. *Macromol. Symp.* **1995**, *91*, 41.
(32) Jacobson, H.; Stockmayer, H. *J. Chem. Phys.* **1950**, *18*, 1600.
(33) Roovers, J.; Toporowski, P. M. *Macromolecules* **1981**, *14*, 1174.
(34) Hadjichrististis, N. *J. Polym. Sci., Part A: Polym. Chem.* **1999**, *37*, 857.
(35) Iatrou, H.; Siakali, E.; Hadjichristidis, N.; Roovers, J.; Mays, J. *J. Polym. Sci., Part B: Polym. Phys.* **1995**, *33*, 1925.
(36) Higgins, J.; Benoit, H. In *Polymers and Neutron Scattering*; Oxford University Press: New York, 19XX; Chapter 6, p 152.
(37) Pedersen, S.; Posselt, D.; Mortensen, K. *J. Appl. Crystallogr.* **1990**, *23*, 321.
(38) Daoud, M.; Cotton, P. *J. Phys.* **1982**, *43*, 531.
(39) Tanaka, T.; Kotaka, T.; Inagaki, H. *Polym. J.* **1972**, *3*, 327.
(40) Zimm, H.; Stockmayer, H. *J. Chem. Phys.* **1949**, *17*, 1301.
(41) Hadjiioannou, G.; Cotts, P.; ten Brinke, G.; Hann, C.; Lutz, P.; Strazielle, C.; Rempp, P.; Kovacs, A. *Macromolecules* **1987**, *20*, 493.
(42) Berne, J.; Pecora, R. *Dynamic Light Scattering*; Wiley: New York, 1976; p 334.
(43) Noolandi, J.; Hong, M. *Macromolecules* **1983**, *16*, 1443.
(44) Ten Brinke, G.; Hadjiioannou, G. *Macromolecules* **1987**, *20*, 486.

MA0121565